LETTERS

Structural mechanism for sterol sensing and transport by OSBP-related proteins

Young Jun Im[1,3], Sumana Raychaudhuri[2], William A. Prinz[2] & James H. Hurley[1]

The oxysterol-binding-protein (OSBP)-related proteins (ORPs) are conserved from yeast to humans[1,2], and are implicated in the regulation of sterol homeostasis[3,4] and in signal transduction pathways[5]. Here we report the structure of the full-length yeast ORP Osh4 (also known as Kes1) at 1.5–1.9 Å resolution in complexes with ergosterol, cholesterol, and 7-, 20- and 25-hydroxycholesterol. We find that a single sterol molecule binds within a hydrophobic tunnel in a manner consistent with a transport function for ORPs. The entrance is blocked by a flexible amino-terminal lid and surrounded by basic residues that are critical for Osh4 function. The structure of the open state of a lid-truncated form of Osh4 was determined at 2.5 Å resolution. Structural analysis and limited proteolysis show that sterol binding closes the lid and stabilizes a conformation favouring transport across aqueous barriers and signal transmission. The structure of Osh4 in the absence of ligand exposes potential phospholipid-binding sites that are positioned for membrane docking and sterol exchange. On the basis of these observations, we propose a model in which sterol and membrane binding promote reciprocal conformational changes that facilitate a sterol transfer and signalling cycle.

OSBP was first discovered as a cytosolic receptor for oxysterols[6,7] that downregulate cholesterol synthesis[8]. The cloning of OSBP (ref. 1) led to the identification of a large family of OSBP-related proteins (the ORPs) with seven members in *Saccharomyces cerevisiase* and twelve in *Homo sapiens* (ref. 2). ORPs are essential for life in eukaryotes. The deletion of all seven ORPs leads to severe defects in sterol and lipid distribution and endocytosis in yeast[3,4], and OSBP is essential for embryonic development in mice (M. Brown, personal communication). All ORPs contain a core OSBP-related domain, and many also contain pleckstrin homology domains, transmembrane regions, endoplasmic-reticulum-targeting FFAT (two phenylalanines in an acidic tract) motifs, GOLD (Golgi dynamics) domains and/or ankyrin repeats[2]. These additional domains localize ORPs by binding to phosphoinositides[9], the endoplasmic reticulum protein VAP (vesicle-associated membrane protein (VAMP)-associated protein)[10] and other targeting signals. The localization of ORPs is dynamic. Oxysterol binding changes the subcellular localization of certain ORPs from the cytosol to the Golgi or endoplasmic reticulum[9,11]. ORPs can bind lipids other than oxysterols, including phosphoinositides and phosphatidic acid[12,13]. OSBP is a cholesterol-sensing regulator of two protein phosphatases—a PTPPBS (protein tyrosine phosphatase PC12, Br7, Sl) family member and the serine/threonine phosphatase PP2A (protein phosphatase 2A)[5].

The structure of full-length Osh4 was determined by multiple isomorphous replacement and refined to an R_{free} value of 23% at 1.5 Å resolution (see Methods; Supplementary Fig. 1; Supplementary Table 1). Osh4 is built around a central antiparallel β-sheet of 19 strands (residues 115–293) that form a near-complete β-barrel (Fig. 1a, Supplementary Fig. 2). The strands of the barrel are pitched at ~45° to its axis. The barrel has structural similarity to the large β-barrels of various bacterial outer-membrane transporters[14] as scored by DALI (ref. 15) (Supplementary Fig. 3). There is no pleckstrin homology domain within the OSBP-related domain[13]. A tunnel with mainly hydrophobic walls runs through the centre of the barrel in a location that corresponds to the pore in bacterial outer-membrane transporters (Fig. 1b). As a soluble β-barrel protein with a hydrophilic exterior and a hydrophobic tunnel in the barrel centre, Osh4 resembles an inside-out porin. Residues 1–29 form a lid that covers the tunnel opening (Fig. 1c, d). The N-terminal domain following the lid (residues 30–117) consists of a two-stranded β-sheet and three α-helices that form a 50-Å-long antiparallel bundle, which runs the entire length of the barrel. The portion of the bundle distal to the lid fills the centre of the barrel, forming a plug at the far end of the tunnel. The proximal portion of the bundle forms one wall of the tunnel by replacing the missing strands of the barrel. There is a large carboxy-terminal region (residues 308–434) following the barrel. The exterior surface around the lid of the tunnel contains six highly conserved basic residues (Fig. 1c; Supplementary Fig. 4).

Sterols bind to Osh4 within the central tunnel of the β-barrel in a head-down orientation. The 3-hydroxyl group of the sterol is buried at the bottom of the Osh4 tunnel, and the side chain touches the inner surface of the lid (Fig. 1e). Although Osh4 has a novel fold, the burial of its ligands in a central hydrophobic tunnel is reminiscent of the structures of other lipid binding and transport proteins. The closest analogy is to the steroidogenic acute regulatory protein (StAR) transport (START) domain proteins MLN64 (ref. 16) and StarD4 (ref. 17) that bind cholesterol, the START-domain-containing protein phosphatidylcholine-transfer protein[18], and the mammalian phosphatidylinositol-transfer proteins[19–21]. In these structures, the ligands are completely sequestered from solution. The yeast Sec14 phospholipid-transfer protein[22] (and its relatives[23,24]), the GM2 activator protein[25], the cholesterol-binding proteins NPC2 (ref. 26) and Scp2 (refs 27, 28), and the glycolipid transfer protein[29] have similar ligand-binding tunnels, although some of these are open at one end[22,25,29]. The structural analogy to other lipid transporters suggested to us that Osh4 might be an ergosterol transporter, and that other ORPs might also transport sterols or other lipids.

The most striking aspects of oxysterol recognition by Osh4 are the absence of direct hydrogen bonds between sterol hydroxyl groups and the side chains of conserved amino acids within Osh4, and the prominence of water-mediated interactions. The 3-hydroxyl group of cholesterol, ergosterol and oxysterols binds to two water molecules and to the side chain of Gln 96 within Osh4. This Gln is part of a

[1]Laboratory of Molecular Biology and [2]Laboratory of Cell Biochemistry and Biology, National Institute of Diabetes and Digestive and Kidney Diseases, National Institutes of Health, US Department of Health and Human Services, Bethesda, Maryland 20892, USA. [3]Department of Life Science, Gwangju Institute of Science and Technology, Oryongdong 1, Bukgu, Gwangju City 500-712, South Korea.

© 2005 Nature Publishing Group

hydrated cluster of polar side chains at the bottom of the Osh4 tunnel (Fig. 1e, g). Trp 46, Tyr 97, Asn 165 and Gln 181 comprise the remainder of the polar cluster at the tunnel bottom, and form water-mediated interactions with the 3-hydroxyl group. The 20- and 25-hydroxyl groups of the respective oxysterols interact with relatively ordered water molecules but not directly with the protein. The 7-hydroxyl group of 7-hydroxycholesterol has no apparent hydrogen bonds to either protein or waters. The 25-hydroxyl group is linked through two water molecules to the conserved Lys-109 side chain, but other oxysterol hydroxyl groups are linked to less-well-ordered water molecules. The lack of direct protein interactions with oxysterol hydroxyl groups in Osh4 contrasts sharply to the specific recognition of 24(*S*),25-epoxycholesterol by a His–Trp pair in the liver X receptor[30], a specific effector molecule for a subset of oxysterols.

The absence of direct interactions between the hydroxyl groups and the protein is difficult to reconcile with the concept that Osh4 is a specific effector of oxysterol signalling. We examined the relative affinities of Osh4 for cholesterol and oxysterols. Cholesterol binds to Osh4 with a K_d of 300 nM (Fig. 2a), as compared to a K_d of 55 nM for the oxysterol with the highest affinity among those tested, 25-hydroxycholesterol (Supplementary Fig. 5). Given the modest difference in affinities between these two molecules, and that cholesterol is far more abundant than oxysterols in mammalian cells, we propose that cholesterol is a physiological ligand for ORPs. We will report elsewhere the results of a study that show Osh4 transports ergosterol, the yeast counterpart of cholesterol (S.R., Y.J.I., J.H.H. and W.A.P., manuscript in preparation).

In the bound conformation of Osh4, the sterol ligands within the complex are inaccessible from the outside. Therefore, a conformational change in Osh4 is required for the uptake and release of sterols. The lid has some of the highest *B* values in the structure (Fig. 3b), which suggests flexibility within this region. After limited proteolysis by trypsin in the absence of ligand, Osh4 is rapidly converted to a stable fragment beginning at residue 28 (Fig. 3a), which corresponds to the end of the lid region (Fig. 3b). Binding of 25-hydroxycholesterol stabilizes this region against proteolysis (Fig. 3a). Sterol ligands stabilize the closed conformation of the lid through direct van der Waals interactions with Trp 10, Phe 13 and the highly conserved residues Leu 24 and Leu 27 (Fig. 1f, g). We were unable to crystallize full-length Osh4 in the absence of ligand, which we attribute to the flexibility of the lid region in the unliganded state. We engineered a 'lidless' Osh4 in which residues 1–29 were deleted and the flexible surface loop 236–240 was replaced by an ectopic dipeptide sequence. Mutation of loop 236–240 does not affect cholesterol binding (data not shown). We determined the structure

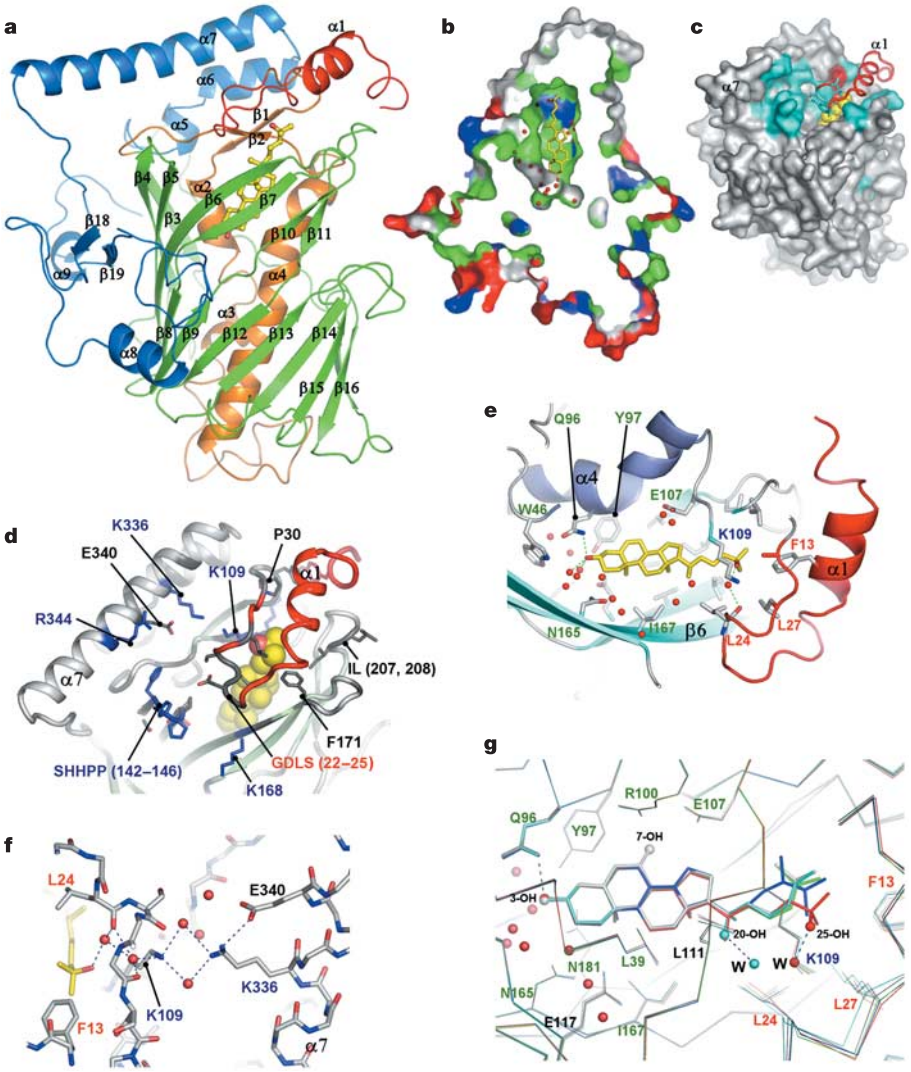

Figure 1 | Structure of Osh4. a, The overall structure of Osh4. The N-terminal lid (residues 1–29) is shown in red, the central helices (30–116) in orange, the β-barrel (117–307) in green and the C-terminal subdomain (308–434) in cyan. The yellow structure is 25-hydroxycholesterol. **b**, The surface of Osh4. Basic residues are shown in blue, acidic residues in red, hydrophobic residues in green and neutral polar residues in white. Water molecules are shown as red spheres. The yellow structure is 25-hydroxycholesterol. **c**, The N-terminal lid of Osh4. Strictly conserved residues are coloured in cyan. The N-terminal lid is shown as ribbons and coloured in red. The yellow structure is 25-hydroxycholesterol. **d**, Tunnel-entrance residues of Osh4. Solvent-accessible conserved residues are clustered around the tunnel entrance. Basic residues are shown in blue, residues within the lid in red, hydrophobic residues (not in the lid) in black. The yellow structure is 25-hydroxycholesterol. **e**, Hydration and hydrogen bonding within Osh4. Residues that bind 25-hydroxycholesterol are coloured in green. Water molecules are shown as red spheres. Hydrogen bonds are shown as dashed lines. The yellow structure is 25-hydroxycholesterol. **f**, Recognition of the 25-hydroxycholesterol 25-hydroxyl group. The ε-amino group of Lys 336 has two conformations in all complexed crystal structures, with the left-hand conformation (closest to Lys 109) predominating. Water molecules are shown as red spheres. Hydrogen bonds are shown as dashed lines. The yellow structure is 25-hydroxycholesterol. **g**, Superposition of five sterols in the Osh4 binding site. 7-Hydroxycholesterol is coloured in grey, 20-hydroxycholesterol in cyan, 25-hydroxycholesterol in red, cholesterol in green and ergosterol in blue, with the respective hydroxyl groups labelled. Water molecules are shown as spheres. Hydrogen bonds are shown as dashed lines. W indicates key water molecules with which the 20- and 25-hydroxyl groups of the respective oxysterols interact.

© 2005 Nature Publishing Group

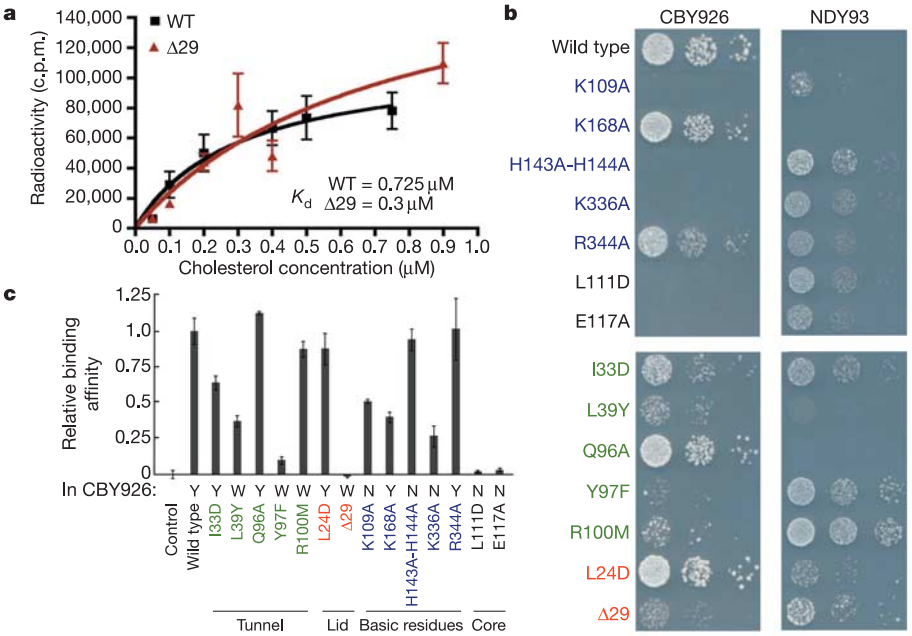

Figure 2 | Mutational analysis of Osh4 binding and function. **a**, Binding curves of cholesterol for wild-type (WT) Osh4 and lid-truncation mutant Osh4 (Δ29) using a low-stringency washing protocol. Each data point shown is the average of two measurements, and the error bars represent the standard errors of the mean derived from the differences between the measurements. **b**, Complementation analysis of wild-type Osh4 and Osh4 mutants. Plasmids encoding Osh4 mutants were introduced into CBY926 (ref. 4) and NDY93 yeast strains. The strains were grown at a permissive temperature (23 °C) and dilution series were incubated at 37 °C. All experiments were repeated at least 3 times with the same results. Expression of mutant proteins *in vivo* was quantified by immunoblotting (Supplementary Fig. 6). **c**, Relative binding affinity of labelled cholesterol (at a concentration of 0.15 μM) for Osh4 mutants relative to wild-type Osh4 (taken as 100%) using a high-stringency washing protocol. The standard error from three measurements is shown by the bars. Y, complements fully; W, complements weakly; N, does not complement.

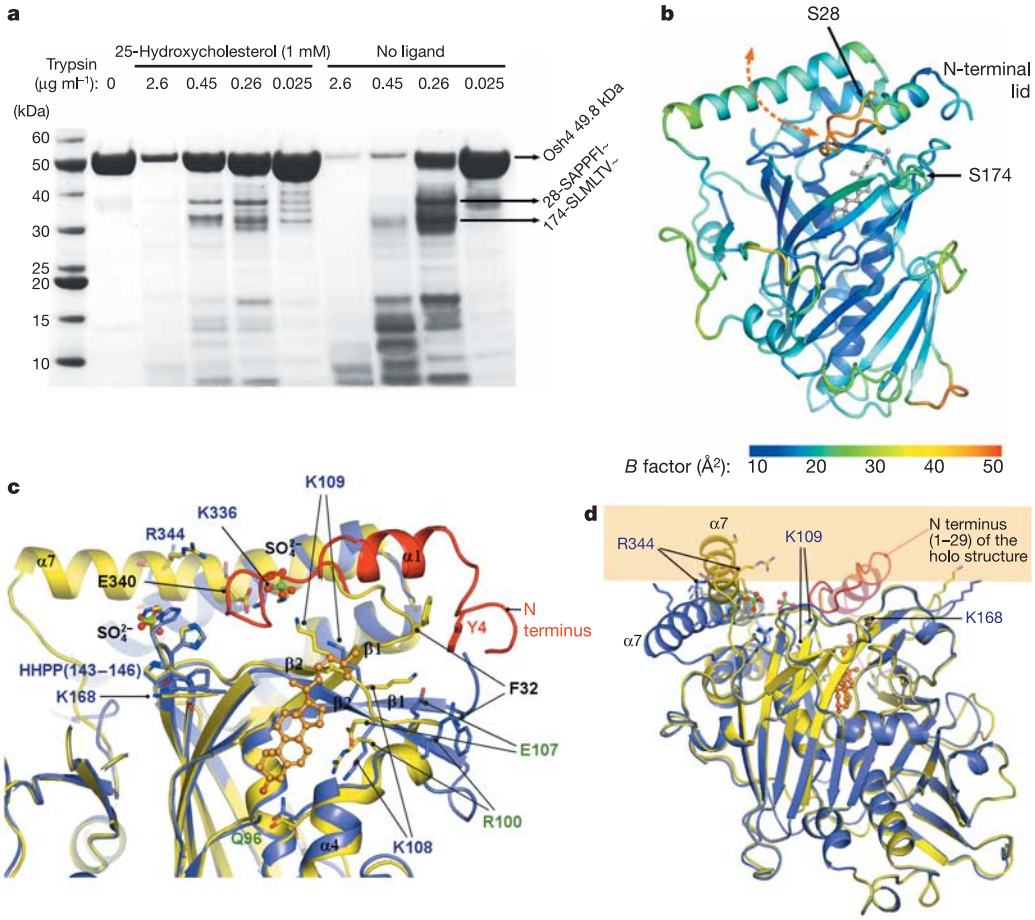

Figure 3 | Conformational changes in Osh4. **a**, Tryptic digestion of Osh4 with increasing concentrations of trypsin. The arrows indicate the N-terminal amino acid sequences of the bands. **b**, The ribbon model is coloured by the average *B* factor of the residues to show their relative mobility. Trypsin cleavage sites are indicated by arrows. The white structure is 25-hydroxycholesterol. **c**, Apo (blue, residues 30–434) and cholesterol-complex (red for the lid region, residues 2–29; yellow for elsewhere, residues 30–434) structures were superimposed. The sulphate ions bound to the apo structure in positions that membrane phospholipid phosphates would bind are shown. The orange structure is cholesterol. **d**, Superposition of apo and cholesterol complex (holo) structures with the location of the membrane indicated by yellow shading. The orange structure is cholesterol.

© 2005 Nature Publishing Group

of this lidless form of Osh4 in its unliganded conformation at 2.5 Å resolution, which we refer to below as the 'apo' structure (Fig. 3c, d).

The apo structure undergoes a dramatic conformational change (2.9 Å r.m.s. for all common Cα positions) compared with the complexed structure. This conformational change is triggered when the ligand–lid interactions are lost. The movement of the lid away from the rest of the protein unlocks helix α7 and basic-residue-containing loops from their complexed conformations. In the apo structure, the tunnel is open and there is no longer any barrier to ligand exchange. Helix α7 pivots about its N terminus such that its C terminus moves 15 Å. The β1 strand and several loop regions near the tunnel opening move by up to 7 Å. The Cα of the conserved basic residue Lys 109 moves 6 Å in this conformational change. These shifts result in the reorganization of the entire conserved basic cluster at the tunnel entrance (Fig. 3c). The apo conformation presents putative phosphate-binding sites and a flattened unobstructed surface surrounding the tunnel opening, which are not present in the bound conformation (Fig. 3d).

We tested whether the conserved basic residues at the tunnel entrance of Osh4, as well as structural core, lid and sterol-binding residues, were important for biological function by assessing their ability to complement a yeast strain in which all seven ORPs have either been deleted, or are present as a temperature-sensitive allele[3]. Lys 109, the His 143–His 144 pair and Lys 336 are essential for function[13], whereas two basic residues that lie further from the tunnel entrance (Lys 168 and Arg 344) are not (Fig. 2b, Supplementary Fig. 6). None of these residues are in direct contact with cholesterol, and their mutation only modestly impairs cholesterol binding (Fig. 2c). In contrast, some mutations within the tunnel (such as Y97F) and structure core mutations near the tunnel (such as L111D and E117A) abrogate both cholesterol binding and biological function (Fig. 2a, c). K109A, K168A and K336A mutations all lead to sharp reductions in basal cholesterol transport by Osh4 (S.R. *et al.*, manuscript in preparation), while H143A-H144A shows a smaller reduction; hence, the major biochemical consequence of mutation within the basic cluster is a consistent defect in sterol transport.

In the complexes, the ε-amino groups of Lys 109 and Lys 336 are ~3.6 Å away from each other, and lie in an unfavourable semi-buried environment (Fig. 1f). In the apo structure, they move 8.7 Å apart.

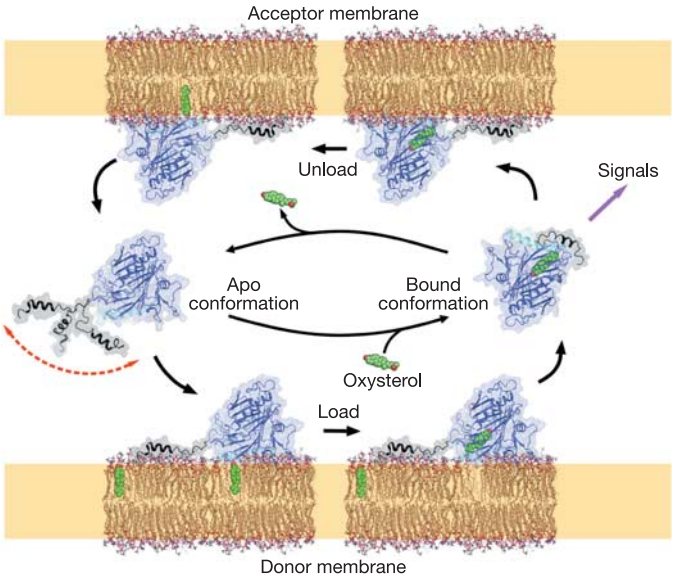

Figure 4 | Mechanism of sterol transfer. The proposed cholesterol transfer cycle is depicted. Oxysterols are shown binding in the cytosol rather than the membrane (as for cholesterol) because of their higher solubility. Cholesterol and oxysterol-dependent signals are shown as occurring through the bound conformation in the cytosol as found for OSBP (ref. 5).

Two ordered sulphate ions are bound in the apo structure: one is bound between the new positions of Lys 109 and Lys 336, and the other near the conserved His pair (Fig. 3c). We believe these sulphate ions mimic the roles of phospholipid phosphate groups because they bind in the position expected for the plane of the membrane surface during sterol exchange. The unfavourable geometry of the Lys 109–Lys 336 pair in the complex suggests that the closed structure is in a destabilized 'tense' state. We propose that the open state is selectively promoted by the availability of phosphate groups at the membrane surface, which bind to these Lys residues only in the open state. Thus, these residues appear to function as an electrostatic spring-loaded lock that controls access to the tunnel. On the basis of these observations, we propose a sterol transfer and signalling cycle (Fig. 4).

OSBP is a cholesterol sensor that regulates phosphatase complexes[5]. 25-hydroxycholesterol antagonizes cholesterol activation. We find that 25-hydroxycholesterol and cholesterol bind to the same site within Osh4 and induce similar gross structural changes. However, 25-hydroxycholesterol is unique among oxysterols in that it forms a water-mediated hydrogen bond with the critical Lys 109 residue. Differences in packing between the side chains of different sterols and the surrounding side chains of Ile 17, Leu 24 and Leu 27 within Osh4 lead to shifts in the lid main-chain position by up 1.5 Å when compared with the cholesterol complex (Supplementary Fig. 7). Within the oxysterol complexes, the 25-hydroxycholesterol structure shows the largest differences from the cholesterol complex. The possible role that these subtle structural changes have in explaining 25-hydroxycholesterol/cholesterol antagonism warrants further study.

The lid region and the basic cluster at the tunnel opening are conserved in all ORPs, whereas parts of the cholesterol-binding site are not well conserved, suggesting that many ORPs might transport non-sterol ligands. The conservation of the lid and basic cluster lead us to believe that the transport cycle will be maintained throughout this protein family. Similarly, cholesterol-dependent signalling will require the same apparatus as cholesterol transfer in order to facilitate the uptake of cholesterol at membranes.

METHODS

Protein expression and purification. DNA encoding Osh4 residues 2–434 was amplified by polymerase chain reaction and subcloned into the *Bam*HI and *Xho*I sites of a pGEX-4T vector modified to contain a tobacco etch virus (TEV) protease recognition site. The glutathione *S*-transferase (GST) fusion protein was expressed in *Escherichia coli* BL21(DE3) cells overnight at 30 °C. The cellular lysate was applied to glutathione sepharose, and the GST removed by digestion with TEV protease in the column. Osh4 was eluted with 500 mM NaCl and 50 mM NaH_2PO_4 pH 7.5, concentrated and then purified on a Superdex 200 column (Pharmacia) in 20 mM Tris-HCl pH 8.0, 100 mM NaCl.

Crystallization. 25-Hydroxycholesterol was prepared in ethanol and added at a final concentration of 1 mM to 15 mg ml^{-1} of protein. Crystals were grown by vapour-diffusion at 25 °C above a reservoir of 100 mM 2-*N*-morpholino-ethanesulphonic acid (MES)-NaOH pH 6.5, 12% (w/v) polyethylene glycol 20,000 over one week. Crystals for complexes with ergosterol, cholesterol, 7-hydroxycholesterol and 20-hydroxycholesterol were similarly grown. Crystals were cryoprotected in reservoir solution supplemented with 20% (v/v) glycerol and flash frozen under nitrogen gas at 95 K. Apo Osh4 crystals were grown in 100 mM MES-NaOH pH 6.0 and 1.6 M ammonium sulphate using micro- and macro-seeding. The apo crystals were cryoprotected in reservoir solution containing 32% (v/v) glycerol. Structure determination is described in the Supplementary Methods.

Tryptic digestion and N-terminal amino acid sequencing. 25-Hydroxycholesterol-bound Osh4 was prepared by adding 25-hydroxycholesterol to a final concentration of 1 mM to a 0.3 mM protein solution. The 25-hydroxycholesterol-bound Osh4 or apo-Osh4 proteins (30 μg) were digested with increasing trypsin concentrations at 37 °C for 2 h. Fragments of the Osh4 protein prepared by limited proteolysis with trypsin were separated by SDS–polyacrylamide gel electrophoresis, transferred to polyvinylidene fluoride membrane, and stained with Coomassie blue R-250. Bands were cut out and the N-terminal amino acids were sequenced using a 492cLC Protein Sequencer (Applied Biosystems).

Ligand-binding assay. For the analysis of mutant Osh4 binding at a single concentration (Fig. 2a), [^{3}H]cholesterol and unlabelled cholesterol were mixed

© 2005 Nature Publishing Group

at a ratio of 1:9 to a final concentration of 10 μM in ethanol. Each reaction was carried out at 22 °C in a final volume of 100 μl of 20 mM Tris-HCl pH 8.5, 30 mM NaCl and 100 pmol Osh4. Cholesterol (15 pmol) was added to the protein solution and incubated for 1 h. HiTrap Q resin (20 μl of 70% (w/v); Amersham) pre-equilibrated with buffer A (20 mM Tris-HCl pH 8.5) was added and incubated for 5 min. The tubes were centrifuged at 13,000*g* for 1 min and washed four times with 1 ml of buffer A. The protein was eluted from the resin with 700 μl of buffer A containing 1 M NaCl. After centrifuging at 13,000*g* for 10 min, 200 μl of supernatant was taken and the radioactivity measured in a liquid scintillation counter. In the low-stringency washing protocol (Fig. 2b), radiolabelled cholesterol (40 pmol) was dried under nitrogen and resuspended in 100 μl of 20 mM Tris-HCl pH 8.5, 30 mM NaCl, 0.05% Triton-X100. Purified Osh4 protein was added to a final concentration of 200 nM and incubated at 30 °C. After incubation for 1 h, 15 μl of HiTrap Q resin was added and the samples were vortexed and left at 22 °C for 5 min. The resin was pelleted by spinning at top speed in a microcentrifuge for 5 min. After three washes with 20 mM Tris pH 8.5, the protein was eluted from the resin with 500 μl of 20 mM Tris-HCl pH 8.5, 1 M NaCl. After centrifugation, the radiolabelled cholesterol in the supernatant was determined by scintillation counting. To determine non-specific binding, 500 μM of unlabelled cholesterol was included in the incubation.

Yeast strains and complementation analysis. Complementation analysis was performed by introducing plasmids encoding mutant Osh4 proteins into either the CBY926 (ref. 4) or NDY63 (MAT***a*** *sec14-3 osh4::kanMX4 ura3-1 his3-11,-15 leu2-5,-112*) yeast strains. CBY926 contains a temperature-sensitive allele of *OSH4* (*osh4-1*) and deletions of the other six *OSH* genes. NDY93 is a *sec14-1 Δosh4* strain that cannot grow at 37 °C if it contains a plasmid encoding a functional Osh4 protein; complementing plasmids prevent NDY93 from growing at 37 °C (ref. 13). To assess complementation, strains containing the various plasmids were plated on synthetic complete dextrose medium minus uracil and grown at 37 °C.

Received 16 March; accepted 9 June 2005.

1. Dawson, P. A., Ridgway, N. D., Slaughter, C. A., Brown, M. S. & Goldstein, J. L. cDNA cloning and expression of oxysterol-binding protein, an oligomer with a potential leucine zipper. *J. Biol. Chem.* **264,** 16798–16803 (1989).
2. Olkkonen, V. M. & Levine, T. P. Oxysterol binding proteins: in more than one place at one time? *Biochem. Cell Biol.* **82,** 87–98 (2004).
3. Beh, C. T., Cool, L., Phillips, J. & Rine, J. Overlapping functions of the yeast oxysterol-binding protein homologues. *Genetics* **157,** 1117–1140 (2001).
4. Beh, C. T. & Rine, J. A role for yeast oxysterol-binding protein homologs in endocytosis and in the maintenance of intracellular sterol-lipid distribution. *J. Cell Sci.* **117,** 2983–2996 (2004).
5. Wang, P., Weng, J. & Anderson, R. G. W. OSBP is a cholesterol-regulated scaffolding protein in control of ERK1/2 activation. *Science* **307,** 1472–1476 (2005).
6. Kandutsch, A. A., Chen, H. W. & Heiniger, H. J. Biological activity of some oxygenated sterols. *Science* **201,** 498–501 (1978).
7. Taylor, F. R., Saucier, S. E., Shown, E. P., Parish, E. J. & Kandutsch, A. A. Correlation between oxysterol binding to a cytosolic binding-protein and potency in the repression of hydroxymethylglutaryl coenzyme-A reductase. *J. Biol. Chem.* **259,** 12382–12387 (1984).
8. Schroepfer, G. J. Jr Oxysterols: Modulators of cholesterol metabolism and other processes. *Physiol. Rev.* **80,** 361–554 (2000).
9. Levine, T. P. & Munro, S. The pleckstrin homology domain of oxysterol-binding protein recognises a determinant specific to Golgi membranes. *Curr. Biol.* **8,** 729–739 (1998).
10. Loewen, C. J. R., Roy, A. & Levine, T. P. A conserved ER targeting motif in three families of lipid binding proteins and in Opi1p binds VAP. *EMBO J.* **22,** 2025–2035 (2003).
11. Ridgway, N. D., Dawson, P. A., Ho, Y. K., Brown, M. S. & Goldstein, J. L. Translocation of oxysterol binding-protein to Golgi-apparatus triggered by ligand-binding. *J. Cell Biol.* **116,** 307–319 (1992).
12. Xu, Y. Q., Liu, Y. L., Ridgway, N. D. & McMaster, C. R. Novel members of the human oxysterol-binding protein family bind phospholipids and regulate vesicle transport. *J. Biol. Chem.* **276,** 18407–18414 (2001).
13. Li, X. M. *et al.* Analysis of oxysterol binding protein homologue Kes1p function in regulation of Sec14p-dependent protein transport from the yeast Golgi complex. *J. Cell Biol.* **157,** 63–77 (2002).
14. Buchanan, S. K. β-Barrel proteins from bacterial outer membranes: structure, function and refolding. *Curr. Opin. Struct. Biol.* **9,** 455–461 (1999).
15. Holm, L. & Sander, C. DALI: a network tool for protein-structure comparison. *Trends Biochem. Sci.* **20,** 478–480 (1995).
16. Tsujishita, Y. & Hurley, J. H. Structure and lipid transport mechanism of a StAR-related domain. *Nature Struct. Biol.* **7,** 408–414 (2000).
17. Romanowski, M. J., Soccio, R. E., Breslow, J. L. & Burley, S. K. Crystal structure of the *Mus musculus* cholesterol-regulated START protein 4 (StarD4) containing a StAR-related lipid transfer domain. *Proc. Natl Acad. Sci. USA* **99,** 6949–6954 (2002).
18. Roderick, S. L. *et al.* Structure of human phosphatidylcholine transfer protein in complex with its ligand. *Nature Struct. Biol.* **9,** 507–511 (2002).
19. Tilley, S. J. *et al.* Structure-function analysis of phosphatidylinositol transfer protein alpha bound to human phosphatidylinositol. *Structure* **12,** 317–326 (2004).
20. Schouten, A. *et al.* Structure of apo-phosphatidylinositol transfer protein alpha provides insight into membrane association. *EMBO J.* **21,** 2117–2121 (2002).
21. Yoder, M. D. *et al.* Structure of a multifunctional protein. Mammalian phosphatidylinositol transfer protein complexed with phosphatidylcholine. *J. Biol. Chem.* **276,** 9246–9252 (2001).
22. Sha, B. D., Phillips, S. E., Bankaitis, V. A. & Luo, M. Crystal structure of the *Saccharomyces cerevisiae* phosphatidylinositol-transfer protein. *Nature* **391,** 506–510 (1998).
23. Meier, R., Tomizaki, T., Schulze-Briese, C., Baumann, U. & Stocker, A. The molecular basis of vitamin E retention: structure of human alpha-tocopherol transfer protein. *J. Mol. Biol.* **331,** 725–734 (2003).
24. Min, K. C., Kovall, R. A. & Hendrickson, W. A. Crystal structure of human alpha-tocopherol transfer protein bound to its ligand: implications for ataxia with vitamin E deficiency. *Proc. Natl Acad. Sci. USA* **100,** 14713–14718 (2003).
25. Wright, C. S., Li, S. C. & Rastinejad, F. Crystal structure of human GM2-activator protein with a novel β-cup topology. *J. Mol. Biol.* **304,** 411–422 (2000).
26. Friedland, N., Liou, H. L., Lobel, P. & Stock, A. M. Structure of a cholesterol-binding protein deficient in Niemann-Pick type C2 disease. *Proc. Natl Acad. Sci. USA* **100,** 2512–2517 (2003).
27. Choinowski, T., Hauser, H. & Piontek, K. Structure of sterol carrier protein 2 at 1.8 Å resolution reveals a hydrophobic tunnel suitable for lipid binding. *Biochemistry* **39,** 1897–1902 (2000).
28. Lopez-Garcia, F. *et al.* NMR structure of the sterol carrier protein-2: implications for the biological role. *J. Mol. Biol.* **295,** 595–603 (2000).
29. Malinina, L., Malakhova, M. L., Teplov, A., Brown, R. E. & Patel, D. J. Structural basis for glycosphingolipid transfer specificity. *Nature* **430,** 1048–1053 (2004).
30. Williams, S. *et al.* X-ray crystal structure of the liver X receptor β ligand binding domain: regulation by a histidine-tryptophan switch. *J. Biol. Chem.* **278,** 27138–27143 (2003).

Supplementary Information is linked to the online version of the paper at www.nature.com/nature.

Acknowledgements We thank T. Levine, V. Bankaitis and M. Brown for discussions and sharing unpublished data, N. DeAngelis for technical assistance, R. Craigie for assistance with protein sequencing, J. Kim for advice on the early stages of this project, G. Miller and H. Shi for collecting synchrotron data, C. Beh and R. Scheckman for yeast strains, F. Dyda for maintaining the home X-ray facility, and the staff of beamline X25, National Synchrotron Light Source, Brookhaven National Laboratory and of SER-CAT, Advanced Photon Source, Argonne National Laboratory for assistance with data collection. This research was supported by the intramural program of the NIDDK. Y.J.I. thanks S. H. Eom for mentoring and support. Y.J.I. was partly supported by the Korea Science and Engineering Foundation. Research carried out at the National Synchrotron Light Source is supported by the US Department of Energy, Division of Materials Sciences and Division of Chemical Sciences. Use of the Advanced Photon Source was supported by the US Department of Energy, Basic Energy Sciences, Office of Science.

Author Information Coordinates have been deposited with the Protein Data Bank with accession numbers 1ZHT, 1ZHW, 1ZHX, 1ZHY, 1ZHZ and 1ZI7. Reprints and permissions information is available at npg.nature.com/reprintsandpermissions. The authors declare no competing financial interests. Correspondence and requests for materials should be addressed to J.H.H. (hurley@helix.nih.gov).

© 2005 Nature Publishing Group

Supplementary Methods

Crystallographic analysis. Native data were collected to 1.5 Å resolution from a single frozen crystal with an ADSC Quantum Q210 CCD detector at beamline X25 at the National Synchrotron Light Source, Brookhaven National Laboratory. The crystals belong to space group C2 with unit cell dimensions of a = 82.60, b = 95.17, c = 65.57 Å, β = 96.81˚. All data were processed and scaled using HKL2000 (HKL Research). Heavy atom derivative data sets were collected with an R-AXIS IV image-plate system attached to a Rigaku rotating-anode generator providing Cu K_α radiation. MIR phasing was carried out using the programs SOLVE [1] at 2.4 Å resolution (Supplementary Table 1) and the phases were extended to 1.8 Å and further improved by RESOLVE. Automatic model building was carried out using the program RESOLVE[2], with which about 50 % of the structure was modeled. The remainder of the model was built manually into the density-modified map using the program O[3]. The refinement was carried out using CNS[4]. The final model, consisting of three residues from expression vector, residues 2-434, 25-hydroxy cholesterol and 267 water molecules, was refined at 1.5 Å resolution to an R factor of 22.1% with a free R value of 23.3 %. The model has no residue to be in a disallowed region of the Ramachandran plot except the two residues in the disordered loop β13-β14. Native data sets for the ergosterol, cholesterol, 7- and 20-hydroxycholesterol complexes were collected using Cu K_α radiation or at beamlines, BM22 and ID22, APS, Argonne National Laboratory. Native data for apo Osh4 was collected at beamline BM22, APS. The apo crystal belongs to space group $P2_1$ with unit cell dimensions a = 93.90, b = 100.85, c = 117.62 Å, β = 91.53˚. The structure of apo-Osh4 was determined by molecular replacement with the program MOLREP [5] using the

structure of 25- hydroxy cholesterol complex as a starting model. The resultant map, showing three molecules in an asymmetric unit, was readily interpretable. The structure was refined using CNS [4]. The final crystallographic R value calculated using data from 50 to 2.5 Å, was 21.3% (R_{free} 24.6%). All structural figures were prepared using the program PyMOL (W. Delano, http://pymol.sourceforge.net/)

Mutagenesis. DNA encoding wild type Osh4 was subcloned into the BamHI and XhoI sites of a p426MET vector. All mutations were carried out using p426MET-*osh4* as a template and appropriate primers based on the protocol from QuikChange Site-Directed Mutagenesis Kit (Stratagene). DNA coding for mutants was subcloned into the modified pGEX-4T vector for expression and purification of mutant proteins. Open reading frames of all mutant genes in pMet426 and the modified pGEX-4T vectors were confirmed by DNA sequencing. The gene for green fluorescent protein (GFP) was inserted before the 5-prime end of Osh4 mutant genes in p426MET to check the expression of the proteins in yeast by immunoblotting.

Quantitative immunoblot. Cells expressing GFP fusions to Osh4p or Osh4p mutants were lysed in 20mM Tris-HCl (pH 7.4), 100mM NaCl in a Bead Beater-8 (Biospec). Proteins were extracted from cells expressing N-terminal fusions of GFP to wild-type or mutant versions of Osh4p. Equal amounts (150μg) of these extracts were separated by SDS-PAGE. Extracts were separated by SDS-PAGE and immunoblotted using anti-GFP antibody (Roche). Immunoblots were quantitated using an Odyssey infrared imager (LI-COR) according to the manufacturers instructions. Expression of K109A could not be quantitated due to poor growth of cells harboring the GFP-Osh4p-K109A mutations, although cells harboring Osh4p-K109A without the fusion grew normally. The K109A

mutant is expressed and purified from E. coli at the same level as wild-type. Note that the fusion with the lowest expression level (L39Y) is partially functional *in vivo*, therefore changes in expression level alone cannot completely explain the non-complementation of other mutants.

Supplementary Figure Legends

Supplementary Figure 1. Experimental electron density

a. 2.2 Å Experimental MIRAS electron density for 25-HC. b-g show simulated annealing omit maps for the following structures: b. Fo-Fc map for Apo structure at 2.5 Å resolution. c. 1.9 Å Fo-Fc map for 7-HC complex. d. 1.7 Å Fo-Fc map for 20-HC complex. e. 1.5 Å Fo-Fc map for 25-HC complex. f. 1.6 Å Fo-Fc map for cholesterol complex. g. 1.9 Å Fo-Fc map for ergosterol complex. Maps are contoured at 2.0 σ, except in (a) at 1.0 σ and (b) at 3.0 σ.

Supplementary Figure 2. Topology of the ORD fold

Domains of Osh4 are shown in the same colors as in Fig. 1a.

Supplementary Figure 3. Comparison to bacterial outer membrane transporters

a. Best-scoring ten structures in the protein data bank as determined by a search with Dali. b. Comparison of the Osh4 structure to the top four structures in the Dali search.

Supplementary Figure 4. Structure-based alignment of ORDs

Amino acid sequences of oxysterol binding domains from seven yeast and twelve human

homologs were aligned based on the structure using the program ClustalX [6]. Conserved residues are colored in dark blue, light blue, and grey, according to their respective degree of conservation from highest to lowest. The r.m.s. main-chain position difference between the cholesterol-bound and apo structures is shown beneath the alignment. Red and green dots below the alignment mark key sterol interacting residues in the lid and in the core of the ORD fold, respectively. Blue dots mark conserved basic residues near the tunnel entrance.

Supplementary Figure 5. 25-hydroxycholesterol binding to Osh4

Data points shown are averages of two measurements, and the error bars show the differences between the measurements.

Supplementary Figure 6. Quantitative immunoblotting

Values obtained are averages from quantitation of two blots and the error bars are derived from the two measurements.

Supplementary Figure 7. Sterol-dependent changes in lid conformation

The superimposed structures of the 25-HC and cholesterol complexes are shown in the vicinity of the lid in the indicated colors.

1. Terwilliger, T. C. & Berendzen, J. Automated MAD and MIR structure solution. *Acta Crystallogr. Sect. D* **55**, 849-861 (1999).
2. Terwilliger, T. C. Automated main-chain model building by template matching and iterative fragment extension. *Acta Crystallogr. Sect. D* **59**, 38-44 (2003).
3. Jones, T. A., Zou, J. Y., Cowan, S. W. & Kjeldgaard. Improved methods for building protein models in electron density maps and the location of errors in these models. *Acta Crystallogr. Sect. A***47**, 110-9 (1991).
4. Brunger, A. T. et al. Crystallography & NMR system: A new software suite for macromolecular structure determination. *Acta Crystallogr. Sect. D* **54**, 905-921 (1998).
5. Vagin, A. A. & Teplyakov, A. MOLREP: an automated program for molecular replacement. *J. Appl. Crystallogr.* **30**, 1022-1025 (1997).
6. Thompson, J. D., Gibson, T. J., Plewniak, F., Jeanmougin, F. & Higgins, D. G. The CLUSTAL-X windows interface: flexible strategies for multiple sequence alignment aided by quality analysis tools. *Nucl. Acids Res.* **25**, 4876-4882 (1997).

Supplementary Table 1

Statistics of data collection, MIR phasing, and crystallographic refinement

Crystal	25-HC complex	TMLA derivative	$HgCl_2$ derivative	$SmCl_2$ derivative	Apo (1-29 deletion)
Heavy atom soaking condition		10 mM, 3days	10 mM, 2hr	10 mM, 2days	
X-ray source	NSLS X25	CuK_α	CuK_α	CuK_α	SER-CAT 22-ID
Wavelength (Å)	1.0000	1.5418	1.5418	1.5418	0.9792
Resolution (Å) (last shell)	1.5 (1.55 - 1.50)	1.9 (1.97 - 1.90)	2.2 (2.28 - 2.20)	1.9 (1.97 - 1.90)	2.5 (2.59 – 2.50)
No. of unique reflections	78130	37805	23391	36446	75120
I/_ (last shell)	54.7 (7.9)	38.2 (7.14)	28.7 (5.16)	40.0 (4.25)	22.9 (3.16)
Rsym [a] (%)	3.8 (20.0)	3.3 (13.5)	5.7 (16.8)	4.3 (19.0)	6.6 (35.5)
Data completeness (%)	97.6 (92.5)	96.5 (81.9)	92.7 (80.1)	91.7 (78.7)	99.3 (96.2)
Phasing and refinement statistics					
Mean FOM (50 - 2.4 Å)			0.61 (SOLVE)		MR
Overall FOM (50 -1.8 Å)			0.72 (RESOLVE)		
R factor [b] (%)	22.0 (27.6)				21.3 (28.7)
Free R factor [c] (%)	23.3 (30.5)				24.6 (33.4)
R.m.s. bond length (Å)	0.005				0.006
R.m.s. bond angle (°)	1.2				1.2
Average B value ($Å^2$) [d] (Ligand)	24.1 (18.6)				50.0

	20-HC complex	7-HC complex	Ergosterol complex	Cholesterol complex
X-ray source	SER-CAT 22-BM	SER-CAT 22-BM	CuK_α	SER-CAT 22-ID
Wavelength (Å)	0.9686	1.0000	1.5418	0.9792
Resolution (Å) (last shell)	1.7 (1.76 - 1.70)	1.9 (1.97 - 1.90)	1.9 (1.97 - 1.90)	1.6 (1.66 – 1.60)
No. of unique reflections	53180	38269	38934	65109
I/σ (last shell)	26.4 (2.4)	16.5 (2.9)	22.4 (5.2)	37.8 (3.6)
Rsym [a] (%)	4.1 (32.6)	5.4 (22.2)	5.2 (28.3)	3.5 (25.5)
Data completeness (%)	97.4 (84.5)	97.1 (85.9)	99.9 (100.0)	98.7 (92.6)
Refinement				
R factor [b] (%)	21.4 (28.0)	21.3 (24.4)	20.7 (24.8)	21.7 (25.3)
Free R factor [c] (%)	23.8 (30.1)	23.9 (28.6)	23.3 (28.0)	23.3 (27.6)
R.m.s. bond length (Å)	0.005	0.006	0.005	0.005
R.m.s. bond angle (°)	1.2	1.3	1.3	1.3
Average B value ($Å^2$) [d] (Ligand)	26.0 (18.6)	22.2 (17.0)	27.9 (21.1)	26.5 (20.2)

The values in parentheses relate to highest resolution shells except for the average B values.

[a] $R_{sym} = \Sigma_h \Sigma_i |I_i(h) - \langle I \rangle| / \Sigma_h \Sigma_i I_i(h)$, where I is the observed intensity and $\langle I \rangle$ is the average intensity of multiple observations of symmetry-related reflections.

[b] $R = \Sigma ||F_o| - k|F_c|| / \Sigma |F_o|$, where F_o and F_c are observed and calculated structure factor amplitudes, respectively.

[c] R_{free} is calculated for a randomly chosen 5% of reflections; the R factor is calculated for the remaining 95% of reflections used for structure refinement.

[d] Average B value of all atoms in an asymmetric unit. The value in parentheses is the average B value of the ligand.

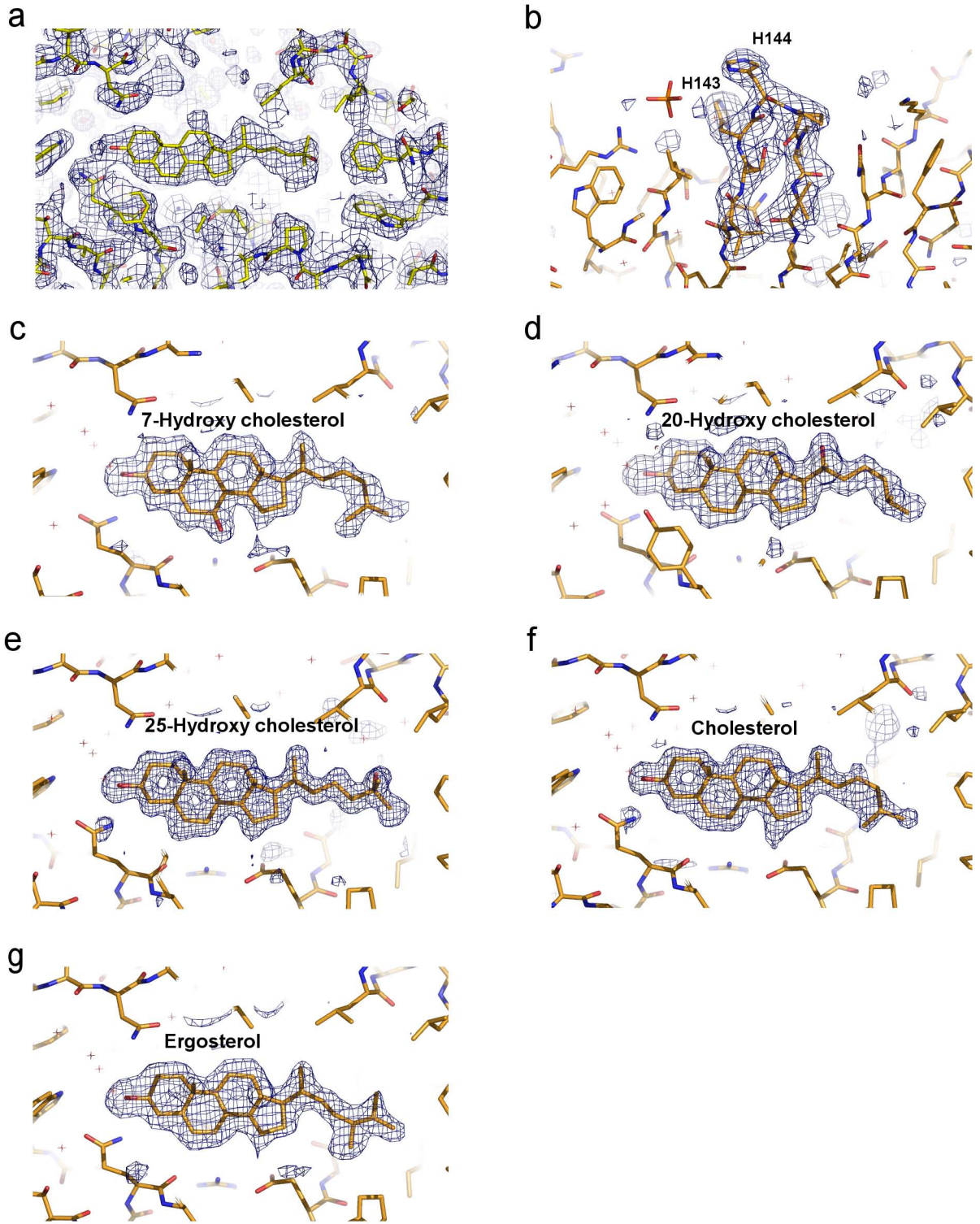
a
b
H144
H143
c
7-Hydroxy cholesterol
d
20-Hydroxy cholesterol
e
25-Hydroxy cholesterol
f
Cholesterol
g
Ergosterol

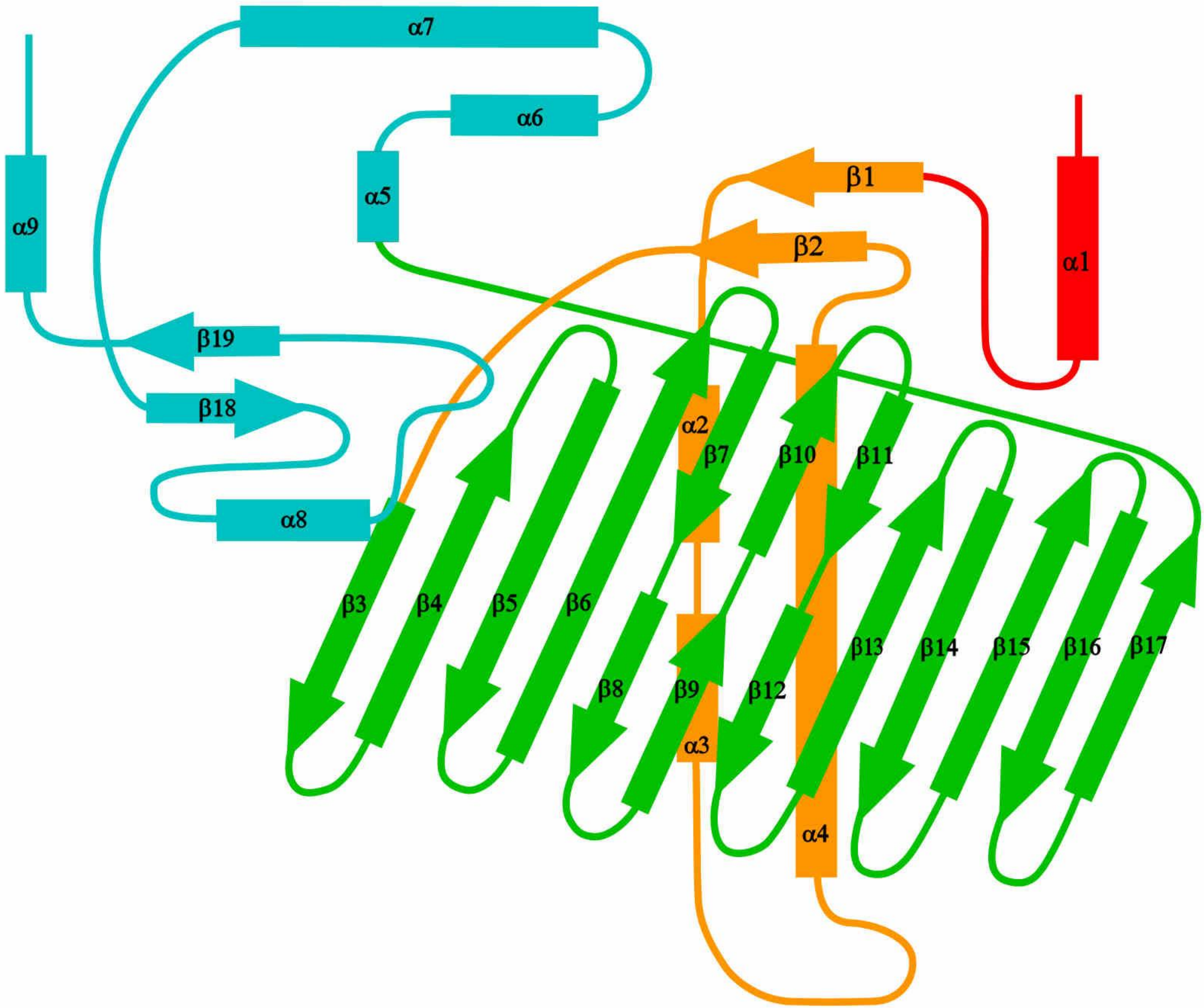
α7
α6
α5
α9
β1
β2
α1
β19
β18
α2
β7
β10
β11
α8
β3
β4
β5
β6
β13
β14
β15
β16
β17
β8
β9
β12
α3
α4

a

NR.	STRID1	STRID2	Z	RMSD	LALI	LSEQ2	%IDE	REVERS	PERMUT	NFRAG	TOPO	PROTEIN
1:	4015-A	2mpr-A	6.2	4.9	153	421	7	0	0	15	S	maltoporin fragment (lam-b, mal-l) biological_unit
2:	4015-A	1kmo-A	6.2	7.6	129	661	8	0	0	12	S	iron(iii) dicitrate transport protein feca (feca)
3:	4015-A	1uyn-X	6.1	3.4	130	279	6	0	0	11	S	nalp (outer membrane protein) fragment
4:	4015-A	1fep-A	6.1	4.3	152	680	7	0	0	17	S	ferric enterobactin receptor (fepa)
5:	4015-A	1nqe-A	6.0	6.0	161	549	4	0	0	20	S	vitamin b12 receptor (outer membrane cobalamin transpor
6:	4015-A	1by5-A	5.9	4.0	130	697	5	0	0	13	S	ferric hydroxamate uptake protein (fhua) ferrichrome
7:	4015-A	1a0t-P	5.4	3.4	139	413	4	0	0	18	S	sucrose-specific porin biological_unit
8:	4015-A	1e54-A	5.3	3.3	122	332	5	0	0	13	S	outer membrane porin protein 32 (omp32) omp32
9:	4015-A	2por	5.2	3.2	129	301	6	0	0	13	S	Porin (crystal form b)
10:	4015-A	2omf	5.2	3.7	137	340	6	0	0	15	S	matrix porin outer membrane protein f (matrix porin, om

b

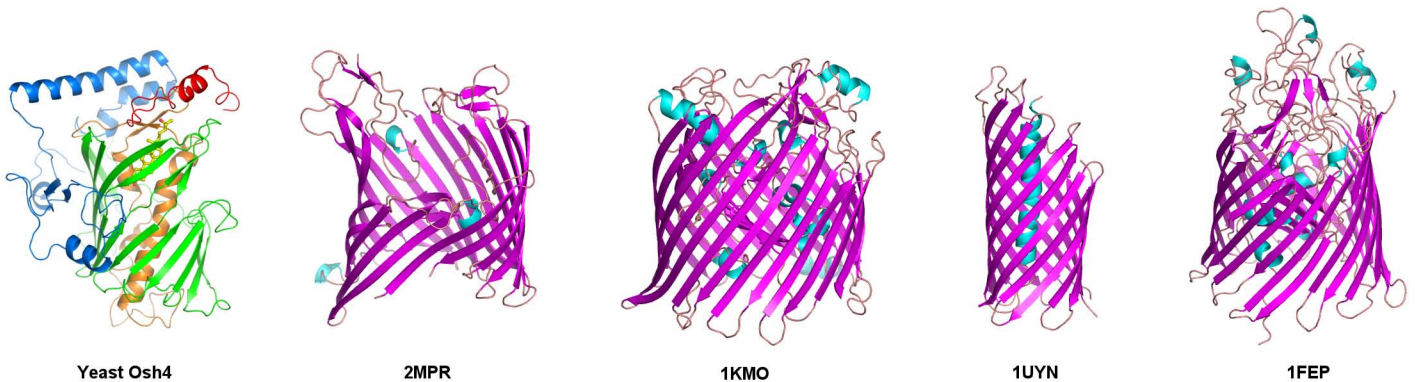

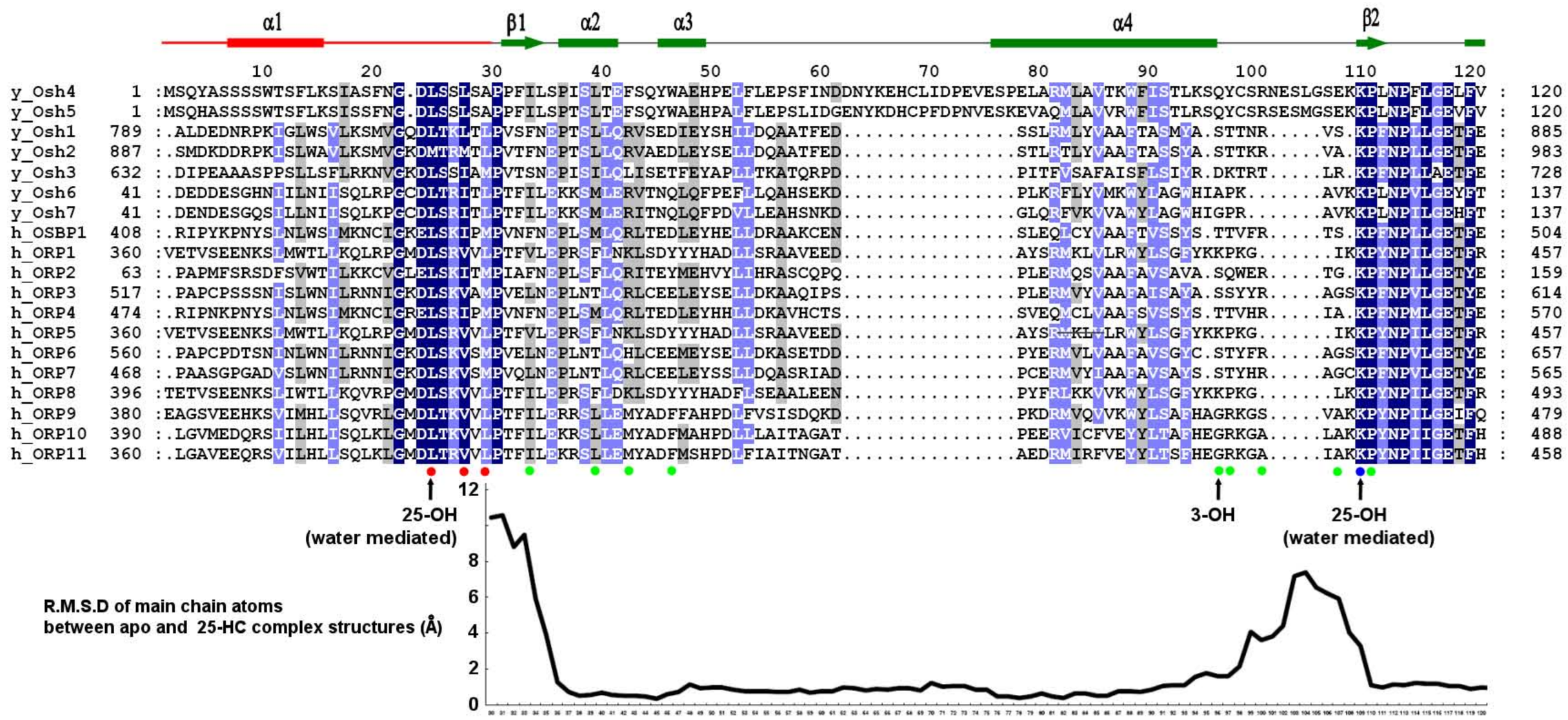
α1
β1
α2
α3
α4
β2
25-OH
(water mediated)
3-OH
25-OH
(water mediated)
R.M.S.D of main chain atoms
between apo and 25-HC complex structures (Å)

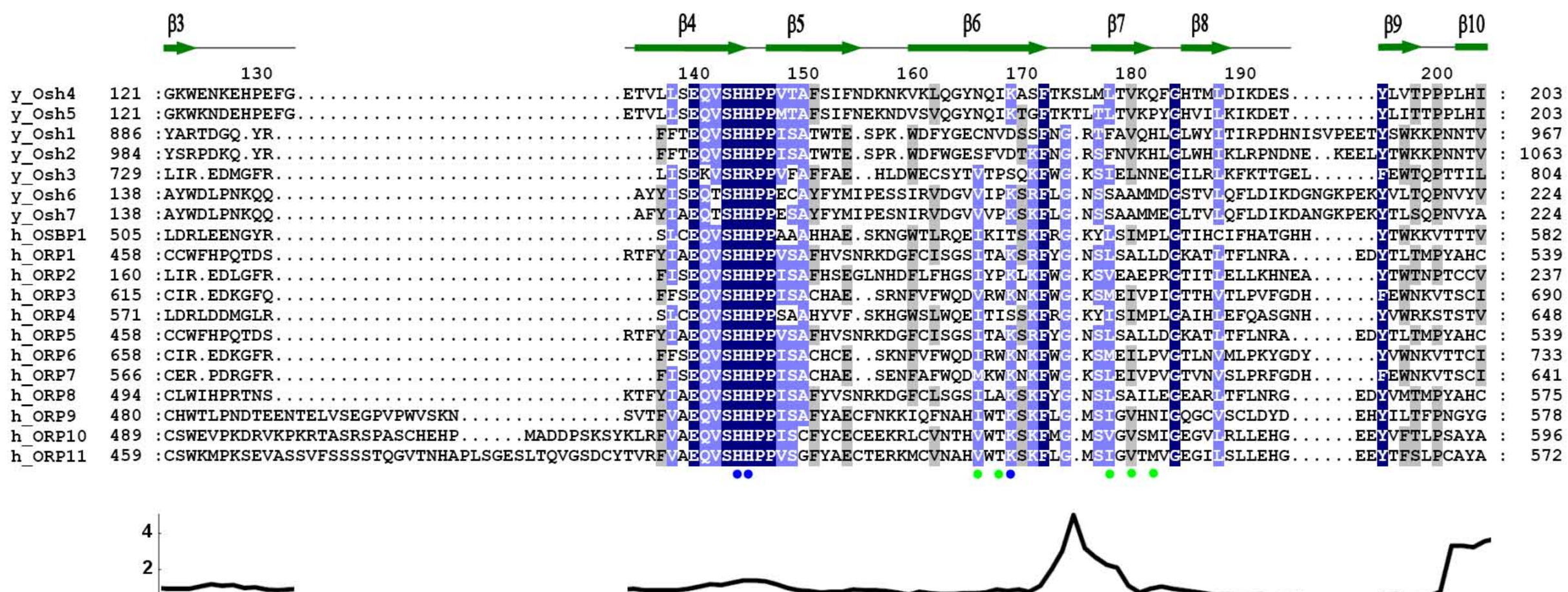
β3
β4
β5
β6
β7
β8
β9
β10

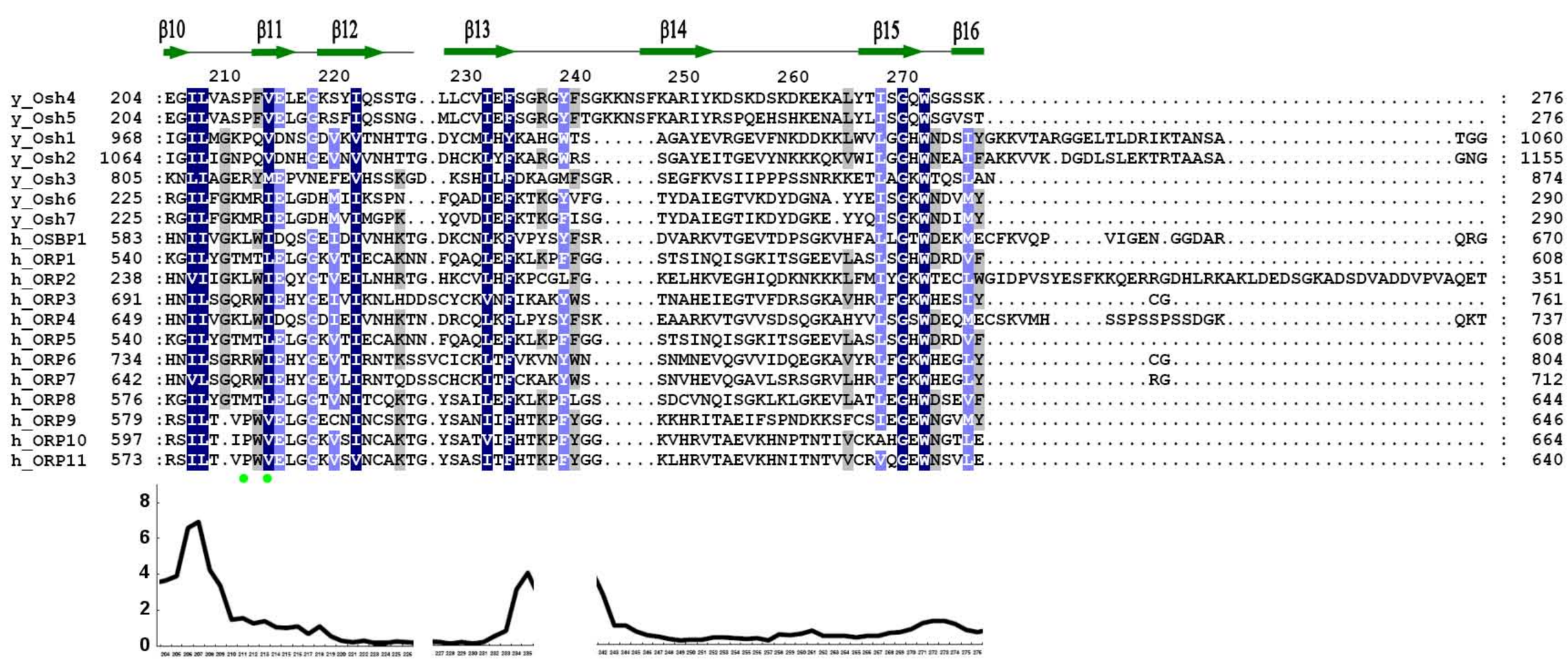
β10
β11
β12
β13
β14
β15
β16

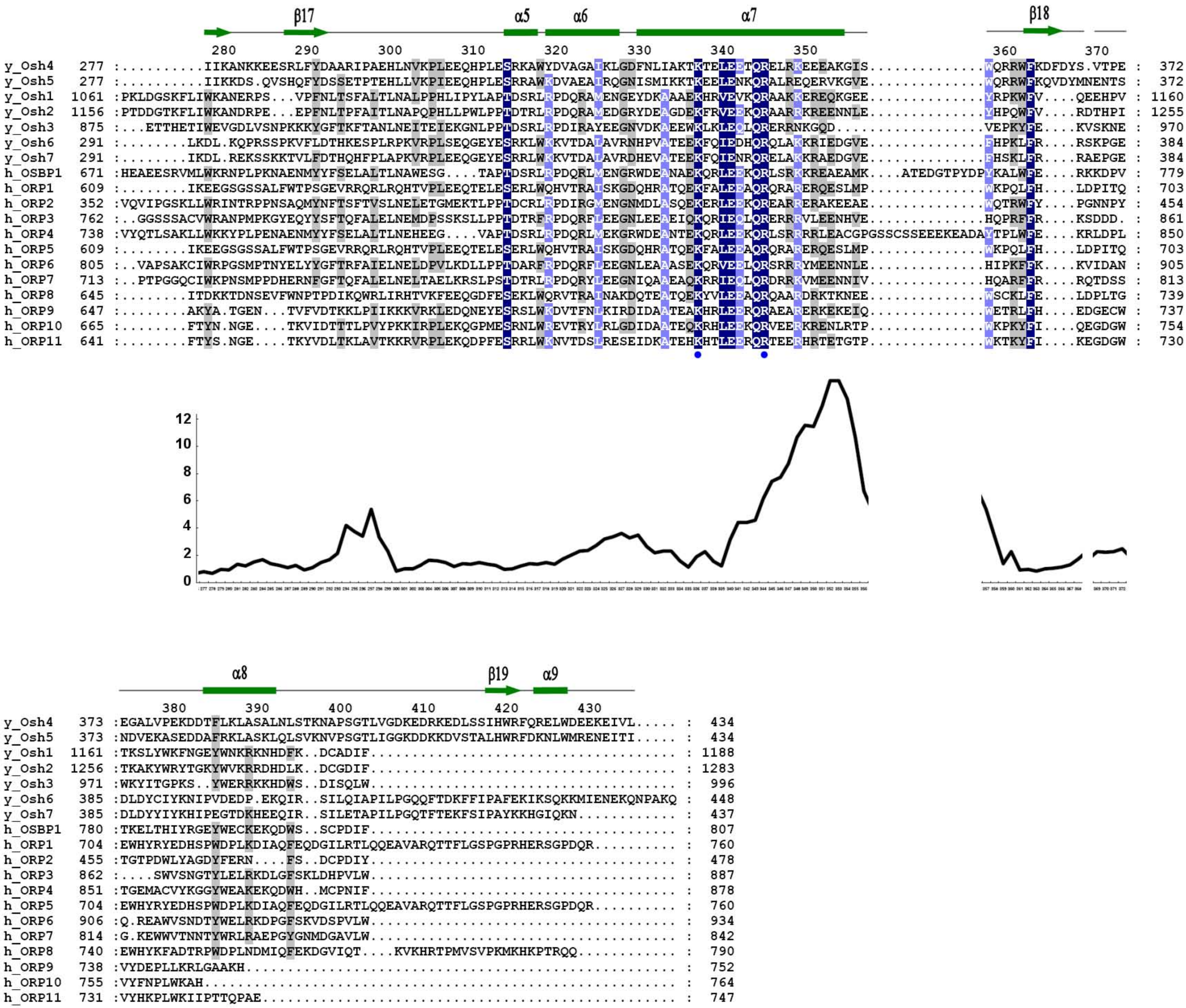
β17
α5
α6
α7
β18
280 290 300 310 320 330 340 350 360 370
y_Osh4 277 :.....IIKANKKEESRLFYDAARIPAEHLNVKPLEEQHPLESRKAWYDVAGAIKLGDFNLIAKTKTELEETQRELRKEEEAKGIS.....WQRRWFKDFDYS.VTPE : 372
y_Osh5 277 :.....IIKKDS.QVSHQFYDSSETPTEHLLVKPIEEQHPLESRRAWKDVAEAIRQGNISMIKKTKEELENKQRALREQERVKGVE.....WQRRWFKQVDYMNENTS : 372
y_Osh1 1061 :PKLDGSKFLIWKANERPS...VPFNLTSFALTLNALPPHLIPYLAPTDSRLRPDQRAMENGEYDKAAAEKHRVEVKQRAAKKEREQKGEE.....YRPKWFV....QEEHPV : 1160
y_Osh2 1156 :PTDDGTKFLIWKANDRPE...EPFNLTPFAITLNAPQPHLLPWLPPTDTRLRPDQRAMEDGRYDEAGDEKFRVEEKQRAARKREENNLE.....YHPQWFV....RDTHPI : 1255
y_Osh3 875 :...ETTHETIWEVGDLVSNPKKKYGFTKFTANLNEITEIEKGNLPPTDSRLRPDIRAYEEGNVDKAEEWKLKLEQLQRERRNKGQD.....VEPKYFE....KVSKNE : 970
y_Osh6 291 :.....LKDL.KQPRSSPKVFLDTHKESPLRPKVRPLSEQGEYESRKLWKKVTDALAVRNHPVATEEKFQIEDHQRQLAKKRIEDGVE.....FHPKLFR....RSKPGE : 384
y_Osh7 291 :.....IKDL.REKSSKKTVLFDTHQHFPLAPKVRPLEEQGEYESRRLWKKVTDALAVRDHEVATEEKFQIENRQRELAKKRAEDGVE.....FHSKLFR....RAEPGE : 384
h_OSBP1 671 :HEAEESRVMLWKRNPLPKNAENMYYFSELALTLNAWESG....TAPTDSRLRPDQRLMENGRWDEANAEKQRLEEKQRLSRKKREAEAMK....ATEDGTPYDPYKALWFE....RKKDPV : 779
h_ORP1 609 :.....IKEEGSGSSALFWTPSGEVRRQRLRQHTVPLEEQTELESERLWQHVTRAISKGDQHRATQEKFALEEAQRQRARERQESLMP.....WKPQLFH....LDPITQ : 703
h_ORP2 352 :VQVIPGSKLLWRINTRPPNSAQMYNFTSFTVSLNELETGMEKTLPPTDCRLRPDIRGMENGNMDLASQEKERLEEKQREARRERAKEEAE.....WQTRWFY....PGNNPY : 454
h_ORP3 762 :..GGSSSACVWRANPMPKGYEQYYSFTQFALELNEMDPSSKSLLPPTDTRFRPDQRFLEEGNLEEAEIQKQRIEQLQRERRRVLEENHVE.....HQPRFFR....KSDDD. : 861
h_ORP4 738 :VYQTLSAKLLWKKYPLPENAENMYYFSELALTLNEHEEG....VAPTDSRLRPDQRLMEKGRWDEANTEKQRLEEKQRLSRRRRLEACGPGSSCSSEEEKEADAYTPLWFE....KRLDPL : 850
h_ORP5 609 :.....IKEEGSGSSALFWTPSGEVRRQRLRQHTVPLEEQTELESERLWQHVTRAISKGDQHRATQEKFALEEAQRQRARERQESLMP.....WKPQLFH....LDPITQ : 703
h_ORP6 805 :..VAPSAKCIWRPGSMPTNYELYYGFTRFAIELNELDPVLKDLLPPTDARFRPDQRFLEEGNLEAAASEKQRVEELQRSRRRYMEENNLE.....HIPKFFK....KVIDAN : 905
h_ORP7 713 :..PTPGGQCIWKPNSMPPDHERNFGFTQFALELNELTAELKRSLPSTDTRLRPDQRYLEEGNIQAAEAQKRRIEQLQRDRRKVMEENNIV.....HQARFFR....RQTDSS : 813
h_ORP8 645 :.....ITDKKTDNSEVFWNPTPDIKQWRLIRHTVKFEEQGDFESEKLWQRVTRAINAKDQTEATQEKYVLEEAQRQAARDRKTKNEE.....WSCKLFE....LDPLTG : 739
h_ORP9 647 :.....AKYA.TGEN...TVFVDTKKLPIIKKKVRKLEDQNEYESRSLWKDVTFNLKIRDIDAATEAKHRLEERQRAEARERKEKEIQ.....WETRLFH....EDGECW : 737
h_ORP10 665 :.....FTYN.NGE....TKVIDTTTLPVYPKKIRPLEKQGPMESRNLWREVTRYLRLGDIDAATEQKRHLEEKQRVEERKRENLRTP.....WKPKYFI....QEGDGW : 754
h_ORP11 641 :.....FTYS.NGE....TKYVDLTKLAVTKKRVRPLEKQDPFESRRLWKNVTDSLRESEIDKATEHKHTLEERQRTEERHRTETGTP.....WKTKYFI....KEGDGW : 730
12
10
8
6
4
2
0

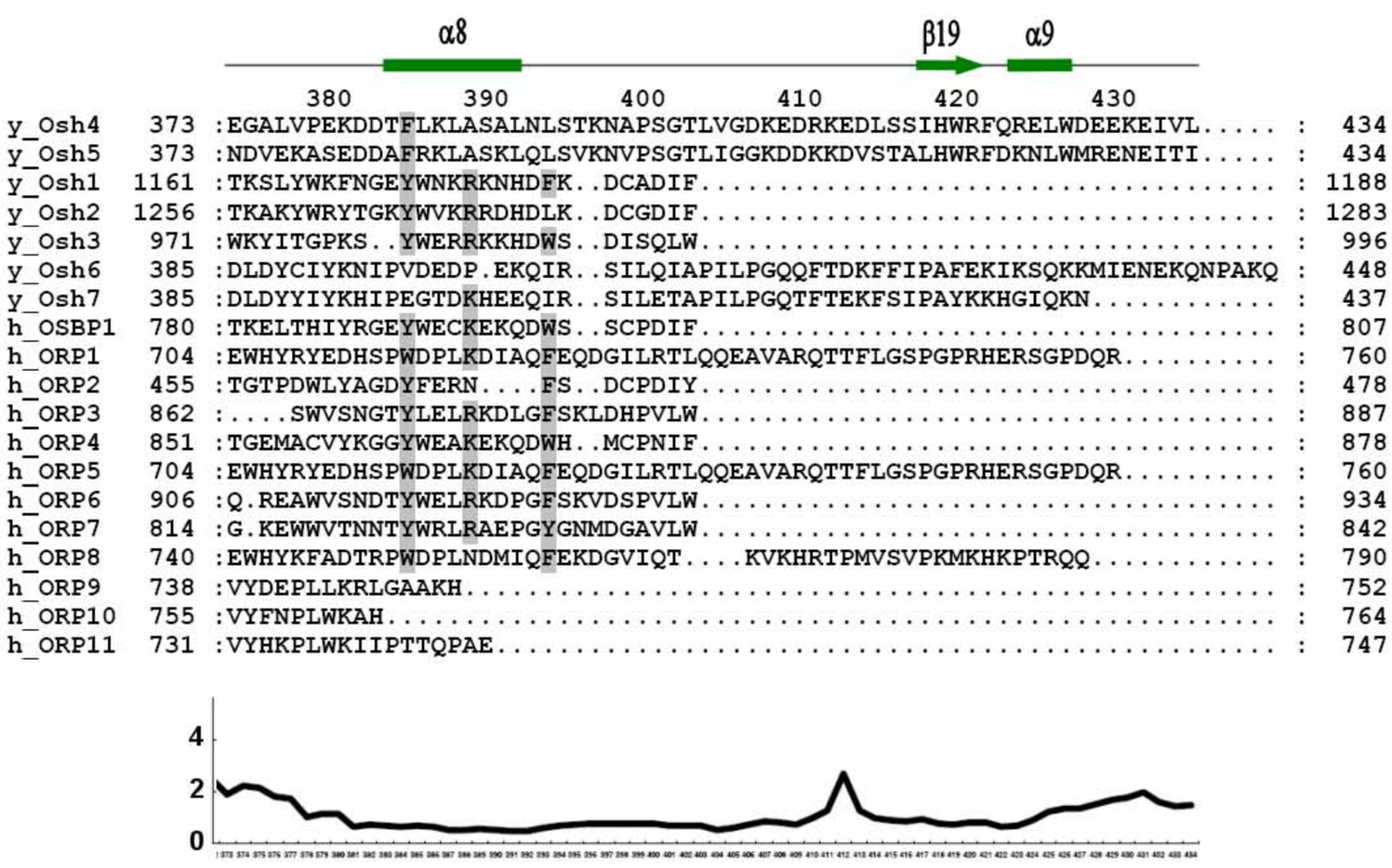
α8
β19
α9
380 390 400 410 420 430
y_Osh4 373 :EGALVPEKDDTFLKLASALNLSTKNAPSGTLVGDKEDRKEDLSSIHWRFQRELWDEEKEIVL..... : 434
y_Osh5 373 :NDVEKASEDDAFRKLASKLQLSVKNVPSGTLIGGKDDKKDVSTALHWRFDKNLWMRENEITI..... : 434
y_Osh1 1161 :TKSLYWKFNGEYWNKRKNHDFK..DCADIF..... : 1188
y_Osh2 1256 :TKAKYWRYTGKYWVKRRDHDLK..DCGDIF..... : 1283
y_Osh3 971 :WKYITGPKS..YWERRKKHDWS..DISQLW..... : 996
y_Osh6 385 :DLDYCIYKNIPVDEDP.EKQIR..SILQIAPILPGQQFTDKFFIPAFEKIKSQKKMIENEKQNPAKQ : 448
y_Osh7 385 :DLDYYIYKHIPEGTDKHEEQIR..SILETAPILPGQTFTEKFSIPAYKKHGIQKN..... : 437
h_OSBP1 780 :TKELTHIYRGEYWECKEKQDWS..SCPDIF..... : 807
h_ORP1 704 :EWHYRYEDHSPWDPLKDIAQFEQDGILRTLQQEAVARQTTFLGSPGPRHERSGPDQR..... : 760
h_ORP2 455 :TGTPDWLYAGDYFERN....FS..DCPDIY..... : 478
h_ORP3 862 :....SWVSNGTYLELRKDLGFSKLDHPVLW..... : 887
h_ORP4 851 :TGEMACVYKGGYWEAKEKQDWH..MCPNIF..... : 878
h_ORP5 704 :EWHYRYEDHSPWDPLKDIAQFEQDGILRTLQQEAVARQTTFLGSPGPRHERSGPDQR..... : 760
h_ORP6 906 :Q.REAWVSNDTYWELRKDPGFSKVDSPVLW..... : 934
h_ORP7 814 :G.KEWWVTNNTYWRLRAEPGYGNMDGAVLW..... : 842
h_ORP8 740 :EWHYKFADTRPWDPLNDMIQFEKDGVIQT....KVKHRTPMVSVPKMKHKPTRQQ..... : 790
h_ORP9 738 :VYDEPLLKRLGAAKH..... : 752
h_ORP10 755 :VYFNPLWKAH..... : 764
h_ORP11 731 :VYHKPLWKIIPTTQPAE..... : 747
4
2
0

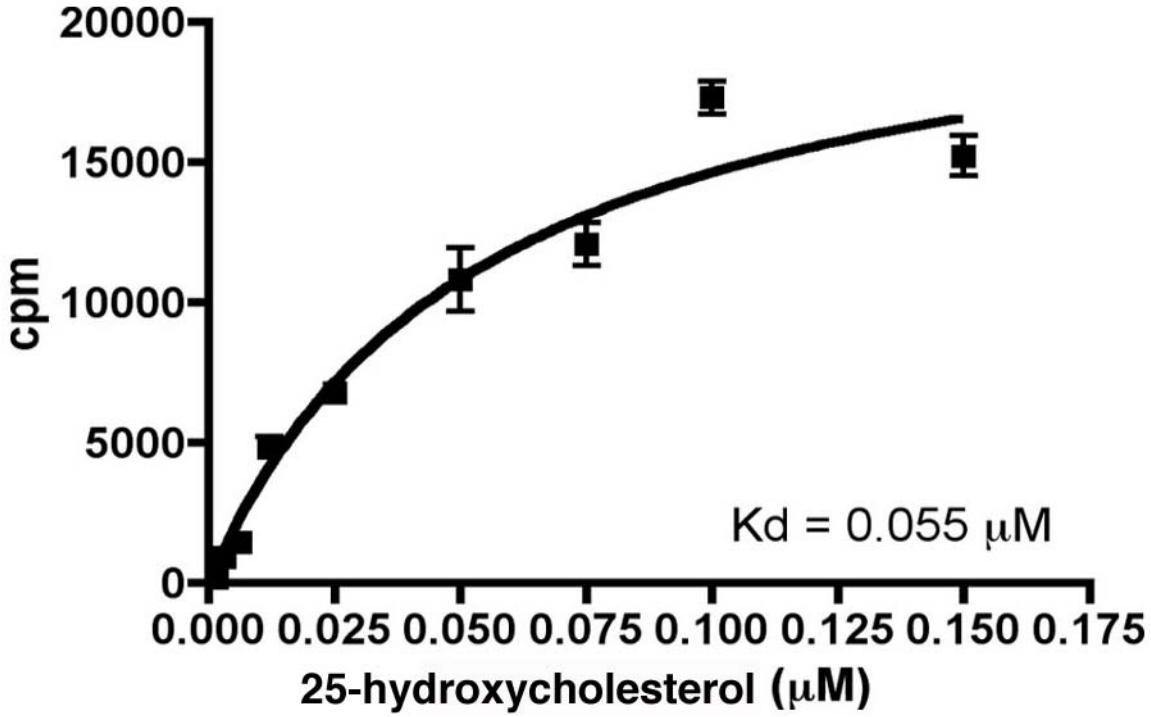
20000
15000
10000
5000
0
cpm
Kd = 0.055 μM
0.000 0.025 0.050 0.075 0.100 0.125 0.150 0.175
25-hydroxycholesterol (μM)

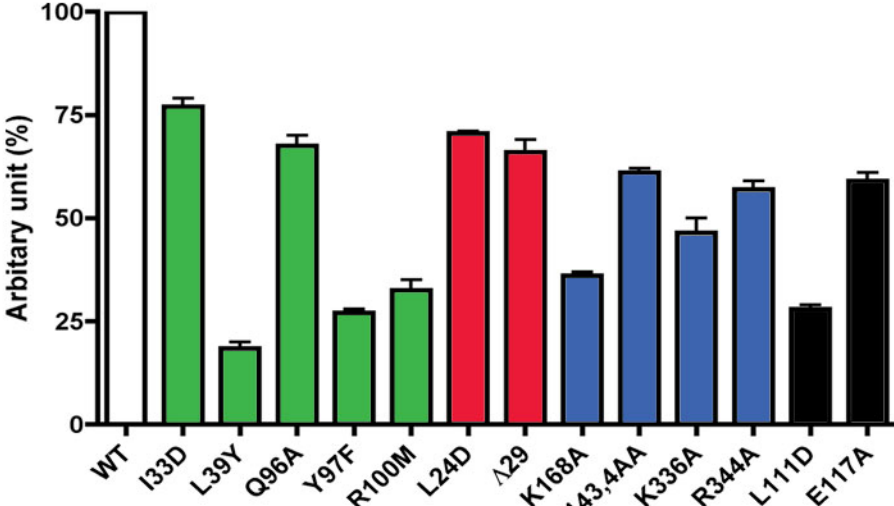
Arbitary unit (%)
100
75
50
25
0
WT
I33D
L39Y
Q96A
Y97F
R100M
L24D
Δ29
K168A
H143,4AA
K336A
R344A
L111D
E117A

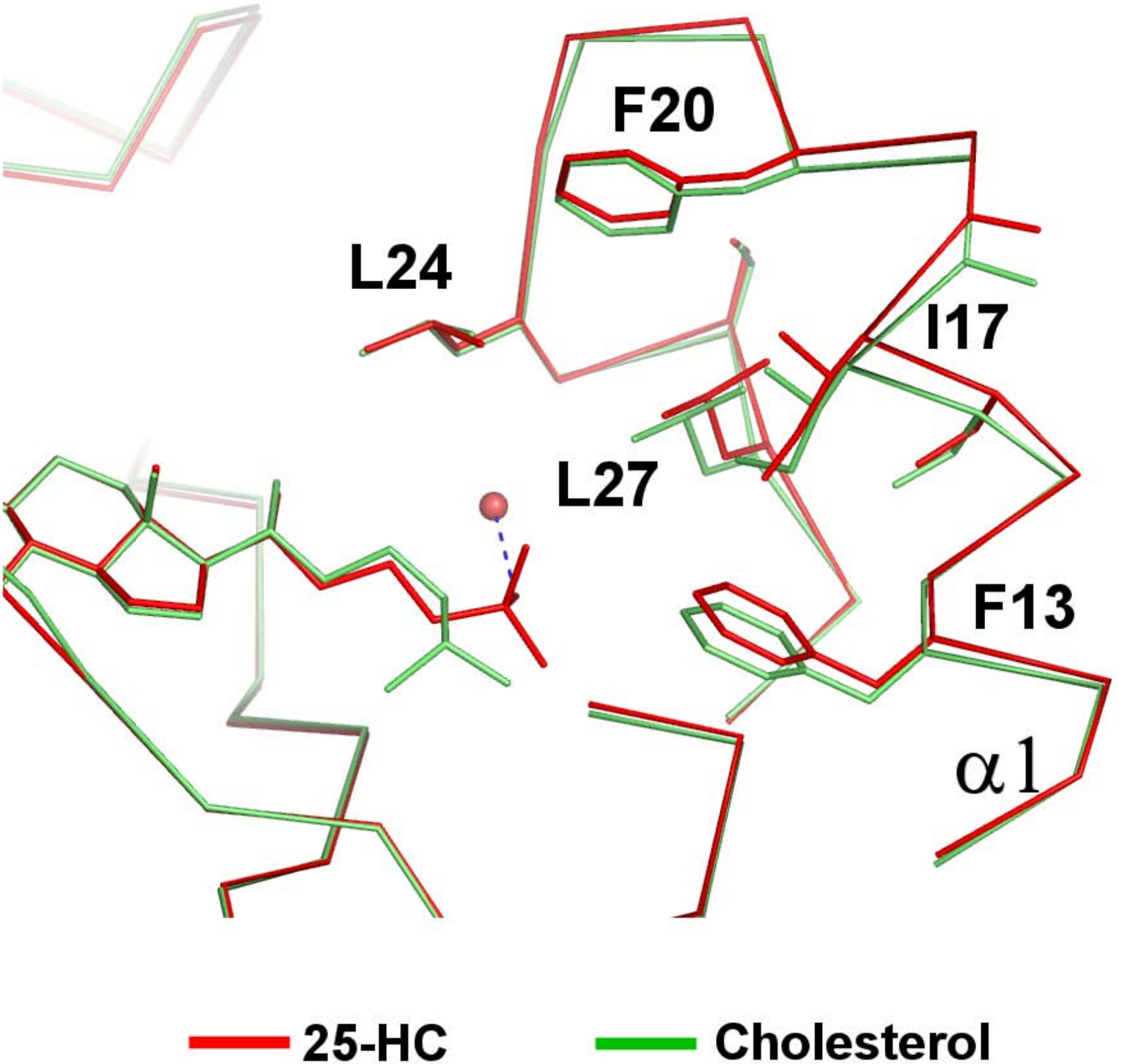
F20
L24
I17
L27
F13
α1
25-HC
Cholesterol